INTERNATIONAL JOURNAL OF CLIMATOLOGY
Int. J. Climatol. (2017)
Published online in Wiley Online Library
(wileyonlinelibrary.com) DOI: 10.1002/joc.5245

RMetS
Royal Meteorological Society

Independently assessing the representation of midlatitude cyclones in high-resolution reanalyses using satellite observed winds

Acacia S. Pepler,[a,b]* Alejandro Di Luca[a,b] and Jason P. Evans[a,b]
[a] *Climate Change Research Centre, University of New South Wales, Sydney, Australia*
[b] *Australian Research Council Centre of Excellence for Climate System Science, Sydney, Australia*

ABSTRACT: High-resolution reanalyses offer the potential to improve our understanding of midlatitude cyclones, particularly smaller-scale systems and those with complex structures. However, previous studies have demonstrated large variations in the frequency and characteristics of Australian midlatitude cyclones between reanalyses when using their native resolution. In this paper we use satellite observations of winds and rainfall in order to evaluate the ability of the ERA-Interim, JRA55, MERRA and CFSR reanalyses to reproduce Australian east coast cyclones. The MERRA reanalysis produces a large number of erroneous small-scale lows without cyclonic wind patterns using a simple pressure-difference-based cyclone identification and tracking method. Consequently, we recommend the ERA-Interim reanalysis when using such methods, or applying more complex tracking methods that are able to compensate for these issues.

KEY WORDS cyclone; wind; rain; satellite; QuikSCAT; TRMM; reanalysis

Received 4 May 2017; Revised 5 July 2017; Accepted 19 July 2017

1. Introduction

Cyclones are important weather systems across the globe and particularly in the midlatitudes, where cyclones and their associated fronts cause the majority of heavy rainfall events (Pfahl and Wernli, 2012; Catto *et al.,* 2015; Utsumi *et al.,* 2017) as well as strong winds (Leckebusch and Ulbrich, 2004). Midlatitude cyclones also play an important role in the global transport of heat and momentum (Chang *et al.,* 2002; Irving *et al.,* 2010) as well as freshwater fluxes into the Southern Ocean (Papritz *et al.,* 2014). For this reason, there is a strong need to understand the frequency, distribution, characteristics and variability of cyclones, with a large number of studies conducted across the world (e.g. Pezza and Ambrizzi, 2003; Allen *et al.,* 2010; Hodges *et al.,* 2011; Neu *et al.,* 2013). The majority of these studies apply an automated program for identifying and tracking cyclones to gridded sea level pressure or geopotential height fields from a global reanalysis. However, several studies have identified large uncertainties in cyclone characteristics between different reanalyses, particularly at higher spatial resolutions (e.g. Hodges *et al.,* 2011; Tilinina *et al.,* 2013; Di Luca *et al.,* 2015). In order to best constrain observed variability as well as develop consistent datasets for evaluation of climate models, it is important to better understand the causes of these variations, as well as which reanalysis might be the best for these purposes.

This paper employs satellite winds and rainfall to provide a detailed assessment of the representation of cyclones across four modern high-resolution reanalyses in a region off the southeast coast of Australia. The cyclones known as East Coast Lows (ECLs) are responsible for the majority of severe weather events on the east coast of Australia and can cause very strong winds, heavy rainfall, widespread flooding, high sea levels, large waves and substantial coastal erosion (Hopkins and Holland, 1997; McInnes and Hubbert, 2001; Callaghan and Power, 2014; Dowdy *et al.,* 2014). For this reason they are an active area of research and the focus of this paper; however, the results presented are expected to be broadly applicable for cyclones beyond this region.

ECLs are frequently defined as cyclones that form or intensify near the east coast of Australia, between 25° and 40°S. This incorporates a broad range of cyclones with different synoptic characteristics, including extratropical cyclones that develop in the midlatitude westerlies and on the wake of passing fronts, subtropical cyclones that develop in a trough near the coast associated with a strong upper-level cut-off low, and decaying or transitioning tropical cyclones (Speer *et al.,* 2009; Browning and Goodwin, 2013). Some develop explosively overnight, when the increased temperature gradient between the continent and warm coastal waters results in enhanced baroclinicity (Holland *et al.,* 1987). Many also have complex characteristics such as daughter cyclogenesis or multiple

* Correspondence to: A. S. Pepler, Climate Bureau of Meteorology, 300 Elizabeth St, Sydney, NSW 2010, Australia. E-mail: acacia.pepler@bom.gov.au

centres, including smaller-scale mesocyclones that can cause locally enhanced rainfall. For this reason, there remains considerable uncertainty as to the 'true' climatology of ECLs, with a number of different databases developed using a range of approaches.

While earlier databases typically relied on subjective identification of ECLs from sea level pressure fields or records of impacts (Holland *et al.,* 1987; Hopkins and Holland, 1997; Callaghan and Helman, 2008; Speer *et al.,* 2009), recent studies increasingly use automated cyclone tracking algorithms to objectively identify ECLs from gridded pressure data (Browning and Goodwin, 2013; Dowdy *et al.,* 2013; Di Luca *et al.,* 2015; Pepler *et al.,* 2015b, 2016). This approach offers a number of advantages, including an increase in the internal consistency of the database and a reduction of human error, as well as the ability to quickly identify cyclones from a large number of data sources such as reanalyses or climate models. However, this approach adds new uncertainties related to the choice of gridded dataset, data resolution, identification method and settings such as threshold intensities (Neu *et al.,* 2013).

Di Luca *et al.* (2015, 2016) applied a consistent cyclone identification and tracking method to a range of high-resolution reanalyses and regional climate model outputs. They identified that, despite broad agreement between reanalyses at a common 300 km resolution, there is considerable uncertainty in the frequency and characteristics of ECLs arising from the choice of reanalysis at finer resolutions. On the native grid, the average annual number of ECLs identified ranged between 22 p.a. using the CFSR reanalysis to over 100 p.a. using the MERRA reanalysis, a fourfold increase. This primarily arose from differences in the frequency of smaller and short-duration cyclones and cyclones during the summer months. The difference in cyclone frequencies between modern era reanalyses have also been identified in global studies (Tilinina *et al.,* 2013; Wang *et al.,* 2016), with MERRA identifying consistently more cyclones across both hemispheres than the other three reanalyses and a larger frequency of shallow or weak cyclones. The differences in frequency and cyclones between reanalyses results in uncertainty when assessing both interannual variability and long-term trends (Eichler and Gottschalck, 2013), as well as in evaluating the output of climate models (Di Luca *et al.,* 2016), so it is necessary to better understand the causes of these differences as well as the most accurate reanalysis to use in future studies.

Following Tilinina *et al.* (2013), Di Luca *et al.* (2015) hypothesized that the difference in the characteristics of cyclones between high resolution reanalyses was due to differences in how the reanalyses solved the equations of state, as well as their cumulus parameterizations. However, as the only 'observational' database available was compiled using daily synoptic charts, and thus did not include potentially true small-scale cyclones, they were unable to recommend a particular reanalysis as closest to the truth.

All datasets of sea level pressure (SLP) are derived from sparse station observations over land, either through direct interpolation or data assimilation into a reanalysis. Consequently, there is no dataset that can be used as ground truth. However, by their nature, cyclones are associated with specific patterns of surface winds and precipitation, with strong differences in both zonal and meridional winds around the cyclone centre and heaviest rainfall poleward of the cyclone centre. Severe ECLs can also be expected to be associated with strong winds and heavy rain. Satellite analyses of wind velocities and rain rate can thus be used as a ground truth for assessing the skill of different reanalyses in generating realistic, impactful ECLs.

In this paper, we will use the Cross-Calibrated Multi-Platform (CCMP) satellite wind speeds (Atlas *et al.,* 2010) between 1988 and 2009, as well as the Tropical Rainfall Measuring Mission (TRMM) satellite rainfall rates (Huffman *et al.,* 2007) between 1998 and 2009, to independently assess four different high resolution reanalyses for their representation of East Coast Lows, and identify the reanalysis with the most realistic cyclones.

2. Data and methods

2.1. Cyclone identification

Six-hourly SLP data at the native (∼0.5°) resolution from four different reanalyses were used to identify ECLs, with the main characteristics of each reanalysis presented in Table 1. The two methods used to identify ECLs from reanalysis data are described below.

2.1.1. The pressure gradient method (PG)

The majority of results in this paper will focus on cyclones identified using the method of Di Luca *et al.* (2015, 2016), for consistency with earlier results. This is based on the method of Browning and Goodwin (2013), and identifies cyclones by searching for a local SLP minima within the ECL region shown in Figure 1. The pressure gradient is then calculated between the cyclone centre and grid points within a 200 km radius of the cyclone centre, with a minimum average pressure gradient threshold of 0.8 hPa/100 km. Once cyclones have been detected, cyclone tracks are constructed by a nearest neighbour search for cyclones in the subsequent 6-hourly analysis, with cyclones assumed to move no faster than 60 km h^{-1}. A minimum average movement rate of 5 km h^{-1} is applied to exclude quasi-stationary anomalies, with a minimum duration of 12 h required to remove any cyclones erroneously identified from short-term fluctuations in SLP.

2.1.2. The Laplacian method (LAP)

As the identification of cyclones is sensitive to the choice of ECL tracking method (Neu *et al.,* 2013; Pepler *et al.,* 2015b, 2016), we compared results using the PG method to ECLs identified using the more complex University of Melbourne cyclone tracking scheme (Murray and Simmonds, 1991; Simmonds and Murray, 1999; Simmonds *et al.,* 1999). This is one of the most widely-used cyclone tracking schemes (Pezza and Ambrizzi, 2003; Pinto *et al.,* 2005; Allen *et al.,* 2010; Irving *et al.,* 2010; Pezza *et al.,*

Table 1. Model type, data assimilation scheme and spatial and temporal resolutions for the four reanalyses used in this paper.

Reanalysis	$\Delta x \times \Delta y$ (°)	Δt (h)	Atmospheric model	Ocean model	Assimilation	Reference
ERAI	0.72×0.72	6	Spectral (T255)	N/A	4Dvar	Dee *et al.,* 2011
JRA55	0.56×0.56	6	Spectral (T319)	N/A	4Dvar	Kobayashi *et al.,* 2015
MERRA	0.67×0.5	1	Finite volume ($0.67° \times 0.5°$)	N/A	3Dvar	Rienecker *et al.,* 2011
CFSR	0.5×0.5	1	Spectral (T382)	Finite difference $0.5 \times 0.5°$	3Dvar	Saha *et al.,* 2010

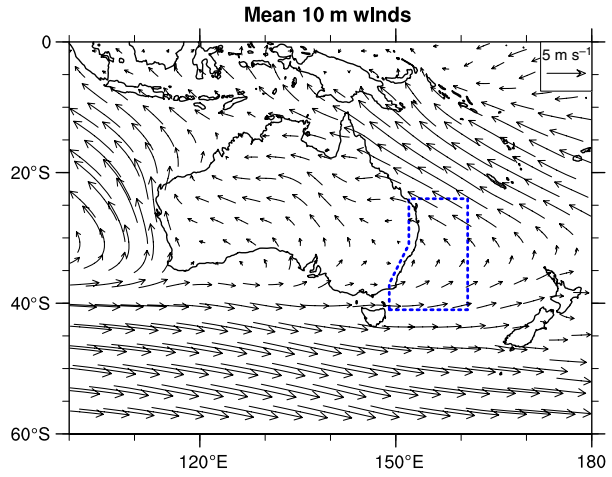

Figure 1. Annual mean 10m wind velocity around Australia in the CCMP satellite dataset. The dashed line indicates the ECL identification region. [Colour figure can be viewed at wileyonlinelibrary.com].

2012; Grieger *et al.,* 2014) and was previously identified by Pepler *et al.* (2015b) as the best method for identifying ECLs when compared to the Speer *et al.* (2009) subjective ECL database.

This method first re-grids the SLP data to a consistent polar stereographic grid, with a spatial resolution of approximately 0.5° at 30°S. As part of this process, SLP is diffusively smoothed using a 0.5° smoothing radius, to reduce the number of erroneous systems generated along trough lines. Cyclones are identified by locating a maximum in the Laplacian of SLP before searching for an associated minimum in the SLP field, with a bicubic spline used to provide sub-gridscale detail. The average Laplacian within a 2° radius of the cyclone centre is then calculated, and only cyclones with an average Laplacian greater than 1.5 hPa $(\text{deg.lat})^{-1}$ retained. The Laplacian of topography is also used to filter spurious cyclones arising from the reduction of pressure to mean sea level. Once cyclones have been identified they are combined into tracks using a probability matching function, with only those ECLs with durations of at least 12 hours and at least one cyclone centre present within the domain in Figure 1 retained for analysis.

To supplement cyclones identified directly from the reanalyses using automated cyclone tracking schemes, we also looked at ECLs identified in the Speer *et al.* (2009) database. This is a subjective database of East Coast Lows between 1970 and 2006, which has since been updated to 2008. ECLs in this database were subjectively identified by skilled observers through visual analysis of the daily 0000UTC hand-drawn synoptic chart prepared by the Bureau of Meteorology's National Meteorological and Oceanographic Centre (NMOC). This dataset allows evaluation of the typical structure of the satellite wind and rain fields for known ECLs; however, this database should not be considered to be 'truth'. In particular, the database is known to exclude fast-moving or rapidly intensifying cyclones due to its low temporal resolution and have issues associated with inconsistent identification of weak cyclones or those near the borders of the domain, while the low spatial resolution of synoptic charts means that small-scale cyclones are likely to be missed (Pepler and Coutts-Smith, 2013).

2.2. Cyclone impacts

Satellite-based wind and rainfall observational datasets were used to evaluate ECLs and their associated impacts.

The Cross-Calibrated Multi-Platform (CCMP) 10-m wind speed data (Atlas *et al.,* 2010) are available 6-hourly in a 0.25° resolution grid mesh over nearly the whole globe (between 78°S and 78°N). CCMP uses a variety of near-surface wind datasets from different sensors and satellites, including SSM/I, TMI, AMSR-E, SeaWinds and QuikSCAT, and they have been calibrated using more than 10 years of 10-m buoy measurements. The CCMP first guess analysis is from ERA-40 between 1987 and 1998 and from the operational ECMWF analysis from 1999. Rainfall rates from the Tropical Rainfall Measuring Mission (TRMM) multi-satellite precipitation analysis 3B42 V7 (Huffman *et al.,* 2007) are available every 3 hours, also on a 0.25° resolution grid.

For each cyclone, the corresponding 10m zonal (u) and meridional (v) winds and the surface precipitation rate within 10° of the cyclone centre are extracted from both the satellite data and the reanalysis fields. These are used to calculate the average wind speed ($w = (u^2+v^2)^{0.5}$) within 5° of the cyclone centre, and the maximum wind speed within 10° of the cyclone centre. The average wind speed is calculated for radii between 1° and 10° from the cyclone centre to identify the radius of maximum winds. We also calculate the average rainfall rates within 2.5° and 5° of the cyclone centre and the maximum rainfall rate within 10° of the cyclone centre. The mean SLP within 10° of the cyclone centre is also composited for each reanalysis. These radii were chosen from inspection of the average pressure and wind patterns around cyclones from the Speer *et al.* (2009) database, with few cyclones having radii of maximum winds greater than 7°.

In the southern hemisphere, cyclonic circulation is clockwise and is indicated by the gradients of wind

around the cyclone centre, with zonal winds expected to be westerly to the north of the centre and easterly to the south ($\Delta u/\Delta x > 0$) while meridional winds are southerly to the east of the cyclone centre and northerly to the west ($\Delta v/\Delta y < 0$). To assess this, for each cyclone and dataset we calculate the zonal difference of the meridional wind (Vdiff) and the meridional difference of the zonal wind (Udiff) at radii between 1° and 7° from the cyclone centre. For example, the meridional difference of zonal wind at a 5° radius is calculated as the difference between the zonal winds averaged over a region within 1° of longitude from the cyclone centre and between 4.5° and 5.5° north of the cyclone centre, minus the zonal winds averaged over a region within 1° of longitude from the cyclone centre between 4.5° and 5.5° south. The maximum difference across the seven radii is used as an indicator of the cyclonicity of the cyclone. Note that the difference in meridional wind has been calculated in the inverse of the normal approach so that positive values indicate cyclonic circulation, i.e. the meridional wind is southerly to the east of the cyclone centre and either northerly winds or weaker southerlies are observed to the west.

To compare cyclones identified between different reanalyses, an individual low is 'matched' if a cyclone is present in the corresponding reanalysis within 5° and 6 hours of the cyclone in the first reanalysis, while an ECL event is 'matched' if this criteria is true for any instance of the ECL. From this, we can calculate the hit rate (HR), false alarm rate (FAR) and the Critical Success Index (CSI), a good index of how similar two datasets are:

$$\mathrm{CSI} = \frac{\mathrm{Hits}}{\mathrm{Hits} + \mathrm{Misses} + \mathrm{FalseAlarms}}$$

3. Satellite observations of subjectively-identified ECLs

Prior to assessing the cyclones identified objectively from reanalyses, we use the Speer *et al.* (2009) subjective database to identify the typical structure of cyclones in the satellite datasets. During the years 1988–2008, the Speer *et al.* (2009) database has an average of 23 ECLs per year. The average duration is slightly under 2 days, with 39 days per year having at least one cyclone identified at 0000UTC. Figure 2 shows the average CCMP wind fields within 10° of the cyclone centre for these events, with cyclonic rotation evident in the u and v fields. The average wind speed is strongest to the south and east of the cyclone centre, with relatively weak winds recorded close to the cyclone centre. Rainfall rates are also highest to the south of the cyclone centre, with relatively low rainfall to the north of the cyclone.

The maximum Udiff and Vdiff within 7° of the cyclone centre were calculated for each cyclone as an indicator of the cyclonicity of the ECL. More than 97% of ECLs had the maximum wind difference greater than or equal to 5 m s^{-1}, with 89% of cyclones exceeding this threshold for both components of the 10 m wind. Those cyclones where this threshold was not reached were manually examined using the corresponding 0000UTC synoptic chart from the NMOC. Several of these were identified as being mis-keyed in the original database, with either the location or the date of the cyclone incorrect, and these errors were subsequently fixed. The remainder of events with wind differences below this threshold were very small cyclones without significant impacts, so no significant events were excluded by this criterion. The average radius of maximum winds across all cyclones in the Speer *et al.* (2009) database is 3.9° and only 10% of cyclones have a radius of maximum winds greater than 7°, typically very small systems where this metric instead detects the stronger winds associated with a more distant cyclone or front, justifying the use of this radius for calculating the cyclonicity of an event.

4. Evaluating reanalyses

4.1. Representation of daily mean winds

The mean CCMP surface wind velocity during the period 1988–2009 is shown in Figure 1. Average wind velocities are small over the ECL region, with generally easterly prevailing winds during the warm months and westerly winds during the cooler months associated with the progression of the subtropical ridge (Timbal and Drosdowsky, 2013; Pepler *et al.,* 2015a). The ERAI reanalysis is able to broadly recreate this pattern, with only small wind anomalies over the ECL region, although the strength of the midlatitude westerlies is stronger than in the satellite data (Figure 3(a)). The other three reanalyses have larger biases, with northerly wind anomalies over the ECL region in MERRA (Figure 3(b)) and CFSR, and to the south of Australia in JRA55. It is important to note here that the improved performance of ERAI could be due to its similarity to the model used as a first guess field for CCMP, rather than to any improvements in its representation of Australian region winds.

As well as assessing their representation of the mean wind fields, we also evaluated the ability of the four reanalyses to represent daily wind patterns over the region 25°–40°S, 152°–160°E for all days between 1990 and 2009. This is the maritime portion of the ECL domain shown in Figure 1, and is used to avoid biasing results over land areas where wind speeds in CCMP are expected to be more strongly influenced by the first-guess analyses.

All reanalyses were bilinearly regridded to the same resolution as CCMP over this domain, and the spatial correlation and RMS error calculated for each day at 0000UTC (Table 2). Both the zonal and the meridional components of wind have spatial correlations greater than 0.9 with the CCMP winds in this region in all four reanalyses, with highest correlations and lowest RMS error for the ERAI reanalysis. The JRA55 and MERRA reanalyses have similar skill, while CFSR is the worst performer on all metrics. ERAI also has the highest correlation and lowest RMSE when calculated only over days when an ECL is identified in the Speer *et al.* (2009) database or when an ECL is identified across all four reanalyses, with CFSR remaining the worst reanalysis (not shown).

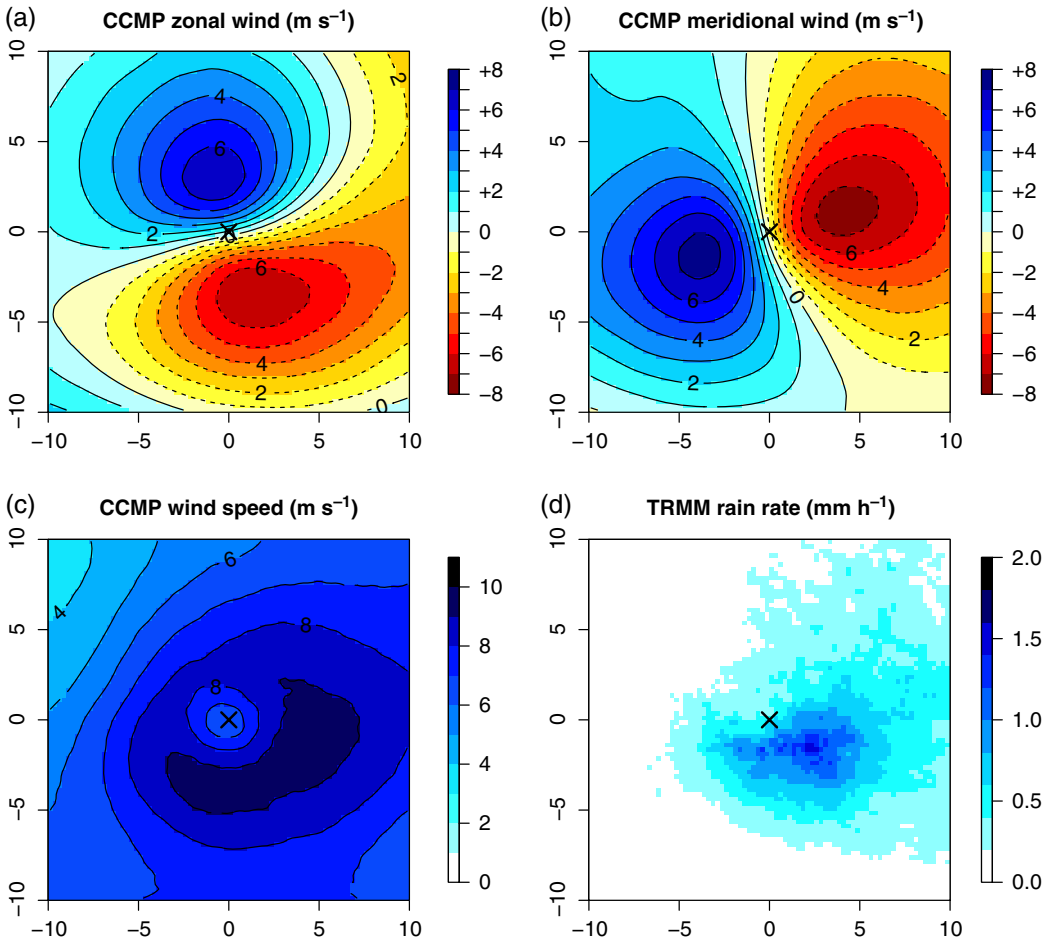

Figure 2. Composite (a) zonal and (b) meridional components of wind and (c) mean wind speed from CCMP within 10° of all ECLs in the Speer *et al.* (2009) database, 1988–2008. (d) Mean TRMM rain rates within 10° of all ECLs in the Speer *et al.* (2009) database, 1998–2008. Cyclones are oriented by cardinal points, and dashed contours indicate negative values. [Colour figure can be viewed at wileyonlinelibrary.com].

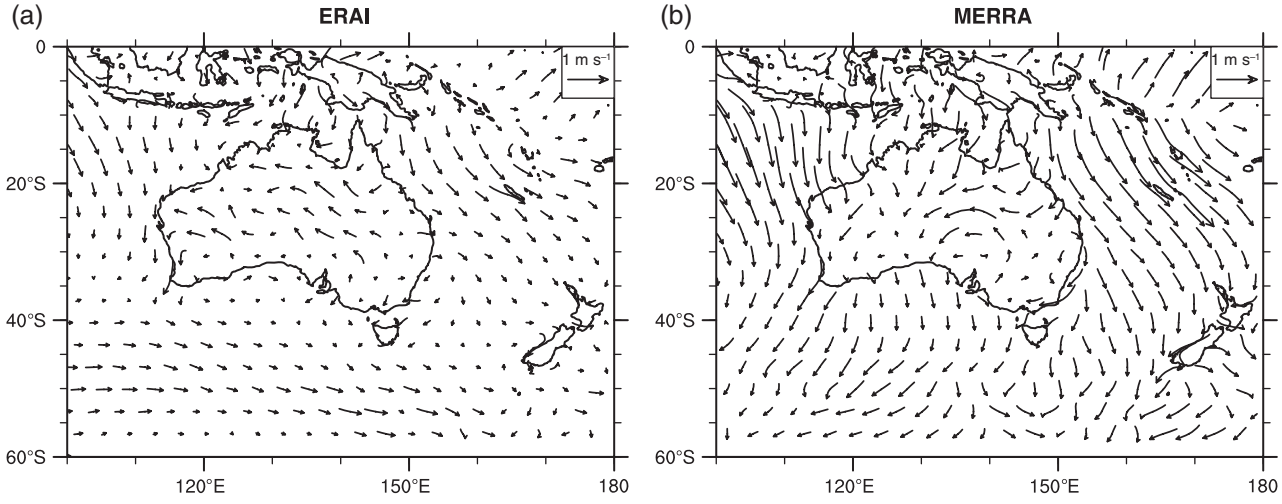

Figure 3. Annual mean 10 m wind velocity anomalies around Australia in (a) ERAI and (b) MERRA, in comparison to the CCMP satellite dataset.

4.2. Representation of winds around known cyclones

We also calculate the average spatial correlation and RMS error for the wind fields within 10° of cyclone centres in the Speer *et al.* (2009) database (Table 3). The RMS error is higher on average during ECLs, which is unsurprising given that the average wind speeds are also higher during ECLs. However, the rankings of reanalyses remain consistent with the results for all days. Figure 4 shows the average bias in the mean winds within 10° of the cyclone centre for all ECLs in Speer *et al.* (2009), with JRA55,

Table 2. Correlation and RMS error of the *u* and *v* components of wind between the CCMP satellite wind data and four reanalysis products over the maritime portion of the ECL domain for all days between 1988 and 2008.

	ERAI	JRA55	MERRA	CFSR
Spatial corr (*u*)	0.96	0.94	0.94	0.92
RMSE (*u*)	1.19	1.49	1.49	1.72
Spatial corr (*v*)	0.97	0.95	0.95	0.93
RMSE (*v*)	1.28	1.56	1.57	1.49

MERRA and CFSR tending to underestimate winds to the west of the cyclone centre and overestimate winds around the centre and further east when compared to CCMP.

The MERRA reanalysis has slightly lower RMS error and higher spatial correlations when we instead assess key features of the cyclone, such as the maximum *U*diff or the average wind speed within 5° of the cyclone centre, although there is little difference in skill between MERRA and ERAI. However, the MERRA reanalysis tends to underestimate both the average wind speed and the average differences of both zonal and meridional wind.

4.3. Representation of ECLs – PG

Consistent with results shown in Di Luca *et al.* (2015), the total number of ECLs when identified using the PG method varies substantially between the three reanalyses (Table 4). Results for CFSR are not shown due to its poor representation of observed winds, but the frequency of ECLs is even lower for this reanalysis, with an average of 8.7 events per year and 15.7 ECL days. Using the intensity threshold chosen, the JRA55 reanalysis is most similar to Speer *et al.* (2009), with fewer ECLs in ERAI and substantially more in MERRA.

It is important to note here that the choice of intensity threshold is intrinsically arbitrary, and this threshold was chosen to allow the best possible comparison to the Speer *et al.* (2009) database across a range of reanalyses. If we restrict analysis to only 0000UTC, consistent with Speer *et al.* (2009) the total number of ECL days drops to 14.6 for ERAI or 40.8 for MERRA. For this reason, previous papers have argued that a weaker intensity threshold is needed to replicate ECLs in the subjective Speer *et al.* (2009) database (Pepler and Coutts-Smith, 2013).

The largest source of difference between the reanalyses is the presence of cyclones where the meridional difference of zonal wind is weak or negative. These form 43% of cyclones in the MERRA reanalysis when *U*diff is derived directly from the reanalysis, or 45% of cyclones when *U*diff is derived from CCMP. The correlation between the *U*diff calculated from CCMP and MERRA is 0.95, so the analysis will focus on results using the difference in the reanalysis itself, as this will better enable future improvements of the tracking scheme. These cyclones are most likely to occur during the warm half of the year, with more than 95% of cyclones in ERAI and JRA55 that fail this criterion, and 81% of MERRA cyclones, occurring between September and March. In comparison, only 56% of cyclones in the Speer *et al.* (2009) database occur during these months, and 61–64% of ECLs in the three reanalyses that satisfy the wind difference criterion.

The average SLP and wind patterns around these cyclones are shown in Figure 5. These are predominantly very small low pressure fluctuations on a trough, northward of a more significant low pressure system. Rather than the cyclonic wind patterns shown in Figure 2, winds are strongest to the east of the cyclone in both MERRA and CCMP. Due to the atypical structure, the average radius of maximum winds for such cyclones is 7.2°, double the radius of 3.7° for cyclones that satisfy the wind difference criterion, while the average size of the cyclone when calculated from the radius of the last closed isobar (Rudeva and Gulev, 2007) is 2.6°, compared to 3.7° for the cyclones that satisfy the criterion. The average rain rate within 2.5° of the cyclone centre calculated from TRMM is also significantly lower, at 0.2 mm h^{-1} compared to 0.7 mm h^{-1} for MERRA cyclones that satisfy the criteria or cyclones identified from Speer *et al.* (2009). For these reasons, we recommend that these cyclones be excluded from analyses, as they are likely to represent small-scale fluctuations in the surface pressure fields rather than true cyclones.

Following the exclusion of cyclones that do not satisfy the wind difference criterion from all datasets the uncertainty in ECL frequency is decreased, with the number of ECL days per year ranging from 23.6 in ERAI to 40.4 in MERRA. On average, the remaining cyclones in MERRA are slightly weaker than the other reanalyses, with weaker average wind speeds and a larger radius of maximum winds (Table 4). However, these are closer to the averages obtained from the Speer *et al.* (2009) database. Furthermore, owing to the greater number of cyclones, the MERRA reanalysis has a higher hit rate when compared to the Speer *et al.* (2009) database, at 64% compared to 50% for ERAI and 54% for JRA55, although the higher

Table 3. Correlation and RMS error of winds around ECLs between CCMP and four reanalysis products, 1988 and 2008.

	ERAI	JRA55	MERRA	CFSR
Spatial corr of *u* within 10° of cyclone centres	**0.96**	0.94	0.95	0.93
RMSE of *u* within 10° of cyclone centres	**1.5**	1.97	1.77	2.22
RMSE of maximum *U*diff	**2.79**	3.17	2.89	3.73
Bias of maximum *U*diff	**+0.10**	+0.58	−0.48	+1.57
RMSE of the average wind speed within 5° of cyclone centres	1.13	1.28	**1.05**	1.30
Bias of the average wind speed within 5° of cyclone centres	**−0.11**	+0.04	−0.31	+0.50

Bold text indicates the reanalysis with highest skill for each metric.

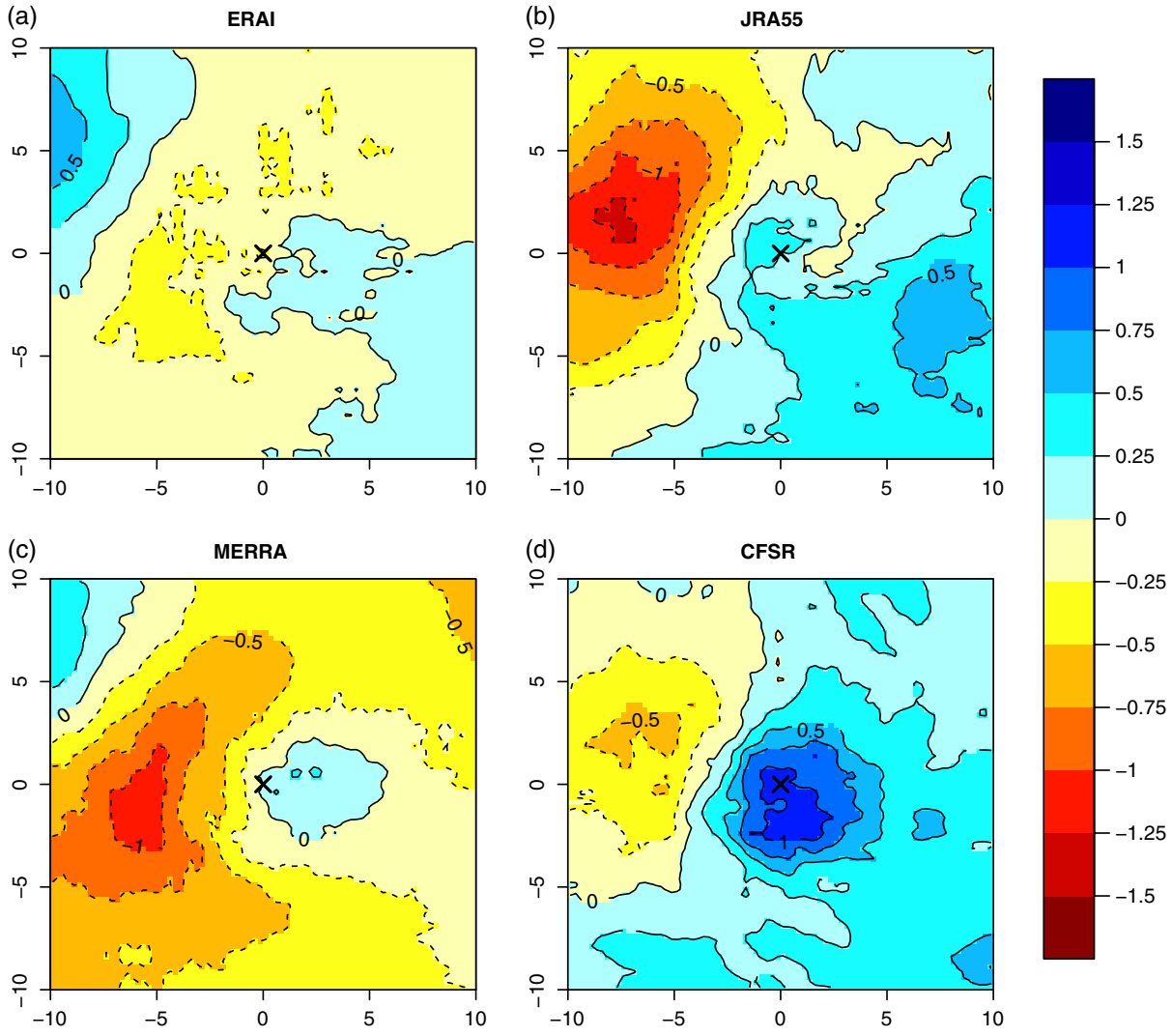

Figure 4. Average difference between the mean reanalysis winds within 10° of all ECLs in the Speer *et al.* (2009) database for four reanalyses, bilinearly regridded to the same resolution as CCMP, and the corresponding winds in CCMP (m s^{-1}). Dashed contours indicate negative values. [Colour figure can be viewed at wileyonlinelibrary.com].

Table 4. ECL statistics as identified from different reanalyses using the PG cyclone identification method, in comparison to the Speer *et al.* (2009) database.

Reanalysis	Speer	ERAI	JRA55	MERRA
ECLs p.a.	20.9	14.8	22	45.6
ECL days p.a.	34.8	24.9	34.7	65.6
% cyclones with maximum *U*diff <5 m s^{-1}	8.3	7.2	15.7	42.8
% cyclones maximum *V*diff <5 m s^{-1}	4.0	0.1	0.8	9.5
Cyclone days if *U*diff<5 are removed	32.0	23.6	29.6	40.4
Average maximum *U*diff (m s^{-1})	15.8	19.2	18.0	15.9
Mean pressure gradient within 200 km of cyclone centre (hPa/100 km)		1.49	1.59	1.58
Mean radius of maximum winds (°)	3.9	2.9	2.8	3.7
Mean wind within 5° of centre (m s^{-1})	8.8	10.0	9.8	8.6

Wind information is obtained from CCMP for the Speer *et al.* (2009) and directly from the reanalysis in other cases, but results are similar if CCMP is used in all cases.

total number of cyclones also results in an increased rate of false alarms.

On average, 31% of ECLs in MERRA are not present in either JRA55 or ERAI. These tend to be weaker cyclones: only 16% of cyclones with mean winds within 5° of the cyclone centre greater than 30 km h^{-1}, or 13% of cyclones with mean rain rates within 2.5° of the cyclone centre greater than 1 mm h^{-1} are unmatched. But unlike the cyclones that failed to satisfy the wind difference criterion in Figure 5, the composite SLP pattern shows a clear low pressure system (Figure 6(a)). Although ERAI does not have a cyclone identified at

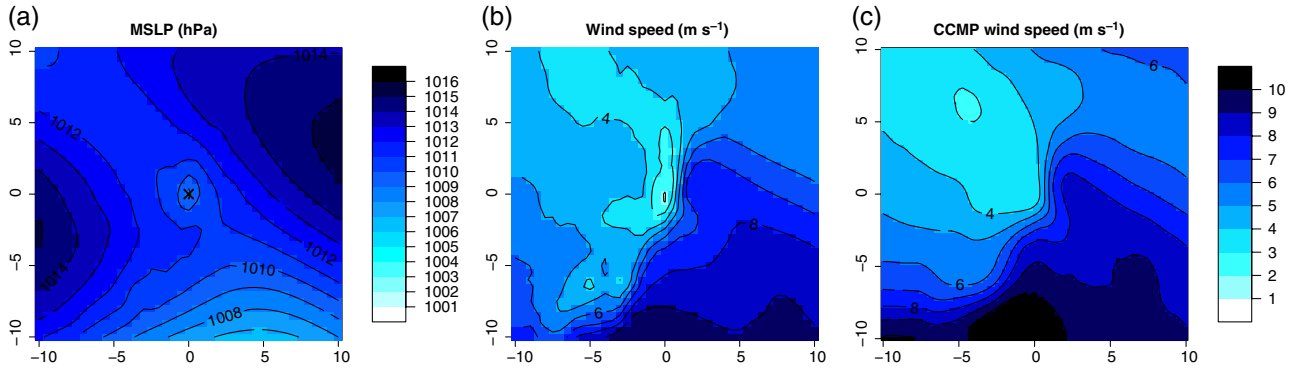

Figure 5. Average (a) SLP and (b) wind speed for cyclones identified in the MERRA reanalysis where the maximum meridional difference of zonal wind is less than 5 m s^{-1}. (c) Corresponding mean wind speed in CCMP. [Colour figure can be viewed at wileyonlinelibrary.com].

these times, it is likely that low pressure systems are present where the average pressure difference does not meet the intensity criterion, as the mean ERAI SLP pattern at these times also shows a clear low pressure system (Figure 6(b)). The average pressure gradient across all ECLs is also slightly lower in ERAI than MERRA or JRA55 (Table 4), which is also the case for matched cyclones.

Figure 7 shows the mean wind speeds for these unmatched cyclones in MERRA, with the corresponding wind speeds from both CCMP and ERAI. Unlike Figure 5, these systems show a clear cyclone centre with decreased wind speeds surrounded by an area of stronger winds, particularly to the south and west of the cyclone, with wind speeds in CCMP similar in magnitude to MERRA. These results suggest that the additional cyclones identified by MERRA are indeed real systems. However, as objective ECL identification relies on the choice of arbitrary thresholds, it may simply suggest that a higher intensity threshold is needed for MERRA to produce similar systems to other reanalyses, which is an approach frequently employed when comparing climate model simulations (Pepler *et al.,* 2016).

4.4. Representation of ECLs – LAP

For comparison with results from the PG method, we also identified ECLs using the University of Melbourne tracking scheme. This has been enhanced with a number of developments including filtering to minimize the occurrence of erroneous cyclones in areas of elevated topography or along trough lines. Consequently, when this method is applied to the three reanalyses with skill at representing observed winds (i.e. excluding the CFSR reanalysis) the variation in cyclone characteristics is smaller, with the total number of ECLs identified varying by less than 25% (Table 5). Notably, more than 95% of ECLs identified using this approach satisfy the criterion for the meridional difference of zonal wind. The difference between the cyclones identified by different reanalyses using the LAP method is also reduced, with CSI scores between the three reanalyses varying between 0.66 and 0.68, compared to 0.42–0.51 for the PG method.

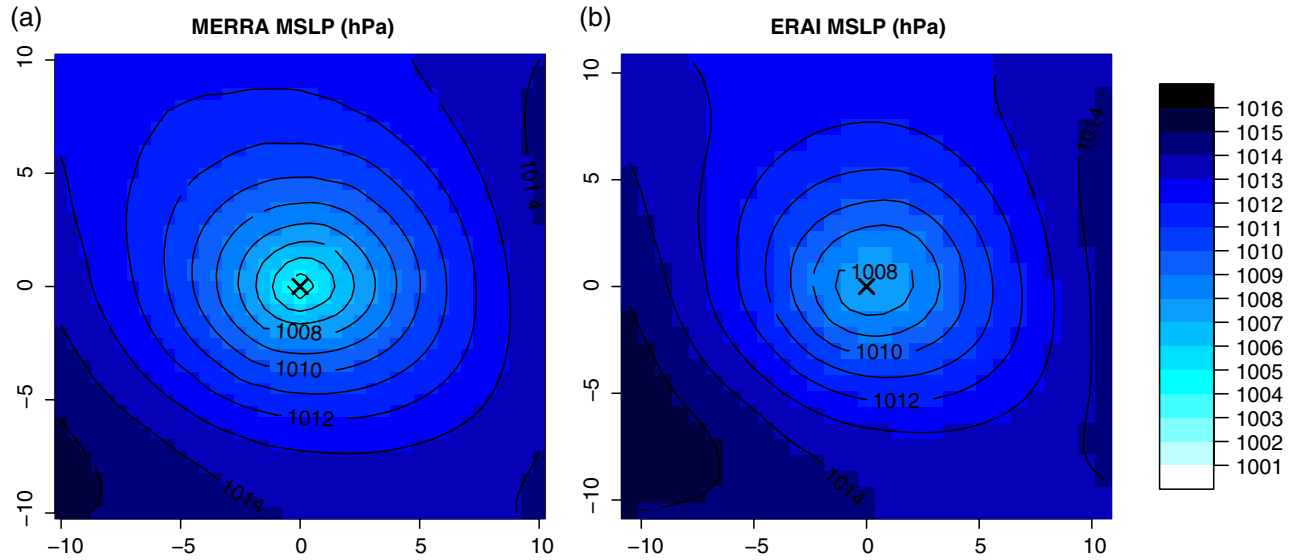

Figure 6. Average mean SLP in MERRA (left) and ERAI (right) within 10° of the cyclone centre for all ECLs in MERRA where *U*diff exceeds 5 m s^{-1} and there is no corresponding cyclone in ERAI within 500 km and 6 h. [Colour figure can be viewed at wileyonlinelibrary.com].

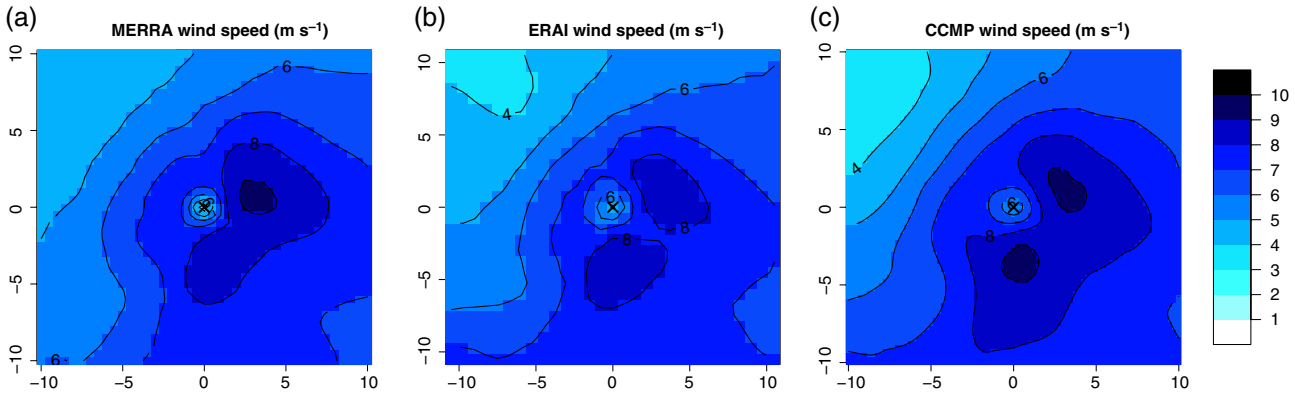

Figure 7. Mean wind speeds in (a) MERRA, (b) ERAI and (c) CCMP within 10° of the cyclone centre for all ECLs in MERRA where the meridional difference of zonal wind exceeds 5 m s^{-1} but there is no corresponding cyclone in ERAI within 500 km and 6 h. [Colour figure can be viewed at wileyonlinelibrary.com].

When comparing ECLs identified in the same reanalysis between the LAP and PG methods, following the removal of all cyclones where *U*diff is less than 5 m s^{-1}, CSI scores range between 0.46 for MERRA and 0.56 for ERAI, with 30% of ECLs in PG-MERRA not detected in LAP-MERRA. This is not simply a result of the different total numbers of cyclones, as 23% of ECLs in PG-MERRA have no matching ECL in LAP-MERRA even using a weaker intensity threshold that gives 53 ECL days per year.

As with cyclones unmatched by other reanalyses, these tend to be weak systems: only 5% of ECLs with mean winds within 5° of the cyclone centre greater than 30 km h^{-1}, or 12% of cyclones with mean rain rates within 2.5° of the cyclone centre greater than 1 mm h^{-1} are unmatched. They are also typically small systems, with an average radius of 2.8° compared to 4.1° for matched systems, while 30% of these cyclones have a radius of maximum winds greater than 7° compared to just 4% of matched cyclones.

Figure 8 shows the average satellite wind speeds and rainfall, as well as SLP from the MERRA reanalysis, for those cyclones in PG-MERRA that do not have a corresponding ECL using the Laplacian method. The CCMP winds show clear cyclonic wind circulation, although this is weaker than for all cyclones, while rainfall is heaviest to the south of the cyclone. These are consistent with the spatial patterns shown in Figure 2, although the magnitude of the winds and rainfall is smaller. The average mean SLP for these systems in MERRA also shows a clear but small cyclone centre, with the combination of reanalysis and satellite data suggesting these are true, but weak, systems that are removed by the Laplacian method.

4.5. ECLs during 2007

To further investigate the characteristics of cyclones identified by the different methods and reanalyses, we performed a manual investigation of the NMOC synoptic charts for all ECLs identified by at least one method in 2007, a year notable for several severe ECLs. During this year there were 32 days with an ECL in the Speer *et al.* (2009) database, equal to the long-term average, and 76 days had an ECL detected in at least one of the three reanalyses and both of the ECL tracking methods.

To minimize issues associated with cyclones close to the boundaries of the domain, we restricted analysis to the region between 27°–38°S, 152°–158°E. In this region there were 47 days where an ECL was identified by one or more datasets, ranging between 17 in LAP-ERAI and 35 in PG-MERRA. 22 days had an ECL present in Speer *et al.* (2009), of which seven were identified by all methods. Three were not identified by either of the automated methods, with only a weak minimum present on the synoptic chart. The remaining ECLs were most likely to be successfully identified using the MERRA reanalysis, with overall hit rates of 68% for LAP-MERRA and 64% for PG-MERRA.

Of cyclones identified by one or more reanalysis that were not present in the Speer *et al.* (2009) database, nine

Table 5. ECL statistics as identified from different reanalyses using the LAP cyclone identification method.

Reanalysis	Speer	ERAI	JRA55	MERRA
ECLs p.a.	20.9	21.2	22.2	25.9
ECL days p.a.	34.8	31.2	31.8	37.1
% cyclones *U*diff <5	8.3	1.2	3.5	1.3
% cyclones *V*diff <5	4.0	0.2	1.3	0.4
Cyclone days if grad <5 are removed	32.0	30.7	30.3	36.5
Average maximum difference of zonal wind (m s^{-1})	15.8	19.7	19.2	19.0
Mean radius of maximum winds	3.9	2.8	2.9	3.0
Mean wind within 5° of centre (m s^{-1})	8.8	10.3	10.5	9.9

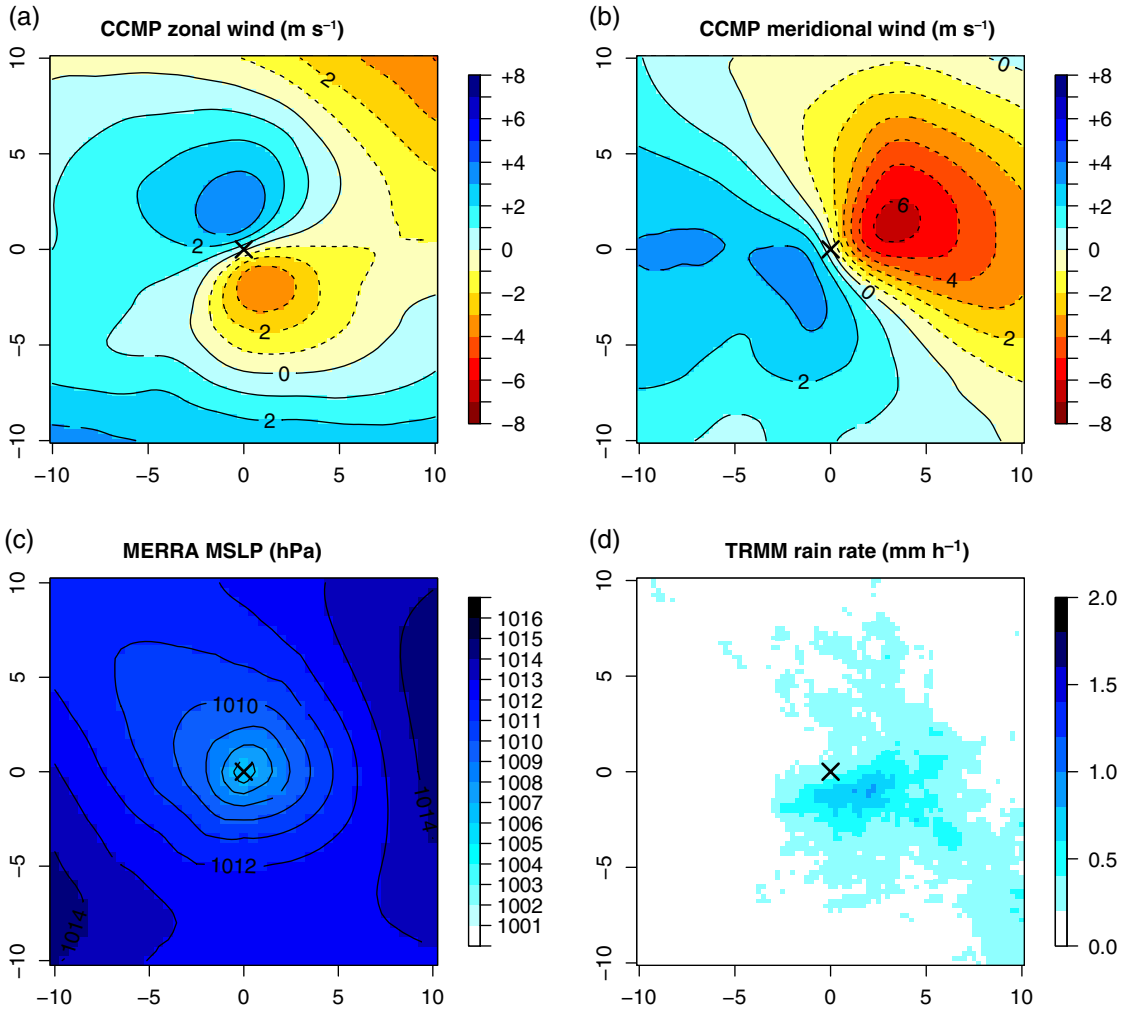

Figure 8. Composite (a) zonal and (b) meridional components of wind from CCMP within 10° for all ECLs in the MERRA reanalysis that are identified by the PG method with *U*diff greater than 5 m s^{-1} but have no corresponding cyclone using the LAP method with a weak intensity threshold. (c) Mean SLP from MERRA reanalysis. (d) Mean TRMM rain rates. Dashed contours indicate negative values. [Colour figure can be viewed at wileyonlinelibrary.com].

were identified by the majority of reanalyses, typically events that underwent rapid development so were not effectively detected using only 0000UTC synoptic charts. The existence of these cyclones further demonstrates the advantage of automated cyclone detection methods over the subjective ECL database. All of these had cyclones present in both PG-MERRA and LAP-MERRA, but were not necessarily present in both ERAI and JRA55.

This leaves 16 days where an ECL was present in only one or two datasets and not present in Speer *et al.* (2009), of which 14 were only present using the PG method and nine only present in PG-MERRA. Manual inspection of the synoptic charts at all of 0000, 0600, 1200 and 1800 UTC showed that these days had, at best, a very small low indicated by an '*x*' on the chart, with several presenting a surface trough with no low pressure centre indicated on the charts at all. Two example charts are shown in Figure 9.

The SLP fields for the three reanalyses corresponding to Figure 9(b) are shown in Figure 10. While the broad patterns are consistent between the reanalyses, both JRA55 and MERRA produce additional fine-scale detail within the surface trough, with local minima near where the '*L*' is marked in the official chart. The contour lines are also less smooth in MERRA, particularly near the elevated topography of the east coast. This small-scale variation makes it susceptible to the generation of erroneous small-scale minima, with the cyclone centre identified by PG-MERRA shown in Figure 9(b).

It is important to note here that the manual surface chart may be missing genuine mesoscale lows. However, of these events, only one had large amounts of rain recorded by the Bureau of Meteorology (http://www.bom.gov.au/jsp/awap, Jones *et al.,* 2009) along the Australian coast in the 24 h to 9am AEDT (~2300UTC) the following day, compared to 45% of ECLs in the Speer *et al.* (2009) database. This was on 31 October 2007, and the rain could equally be attributed to the associated surface trough and onshore flow triggering thunderstorms and showers.

Of the 12 days that were in PG-MERRA but not PG-JRA or PG-ERAI, only one had mean winds within 5° of the cyclone centre greater than 30 km h^{-1} in CCMP,

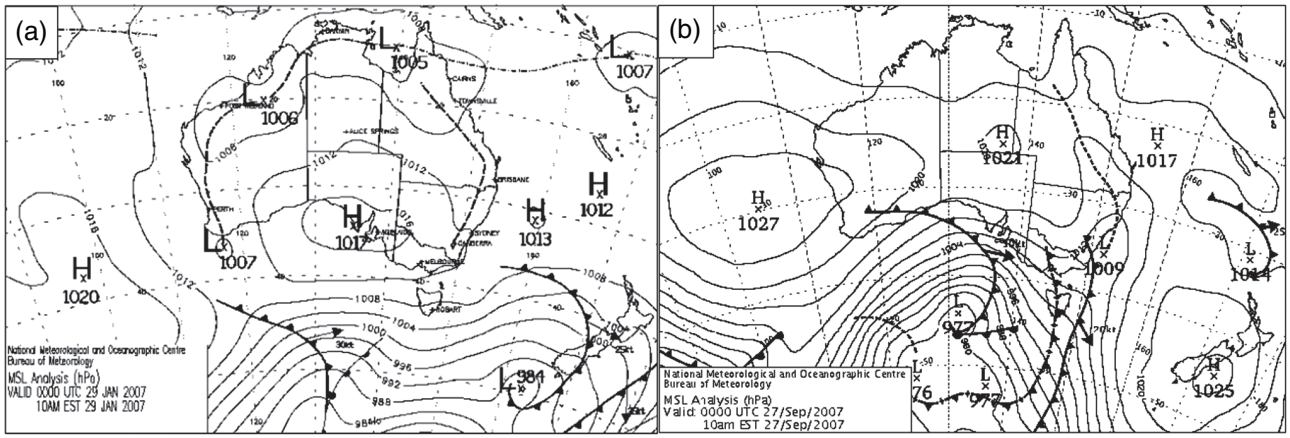

Figure 9. Bureau of Meteorology synoptic charts for two instances where an ECL is only identified by PG-MERRRA: (a) 0000UTC 29 January 2007, (b) 0000 UTC 27 September 2007.

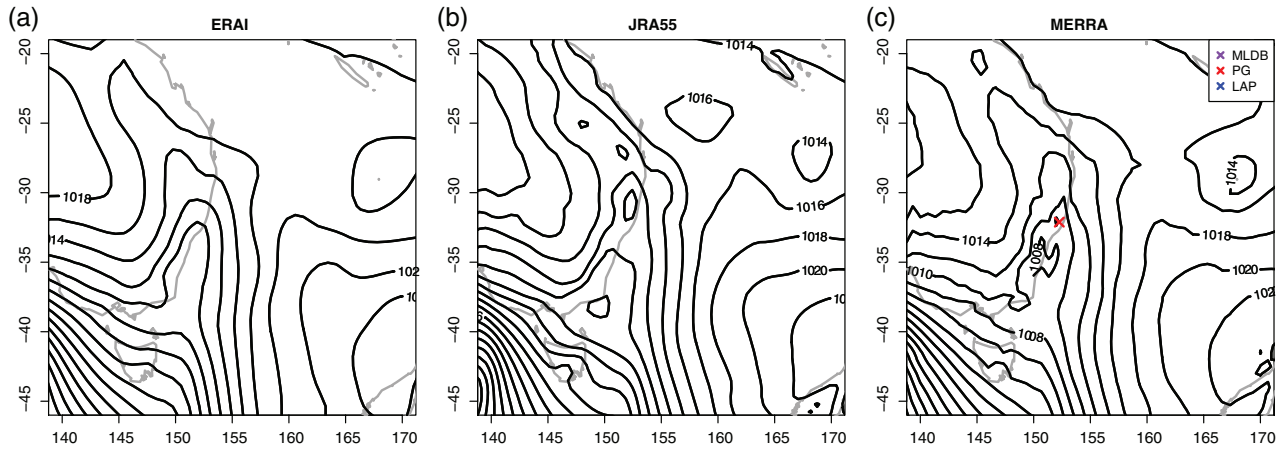

Figure 10. SLP fields at 0000 UTC on 27 September 2007 from (a) ERAI, (b) JRA55 and (c) MERRA. Crosses indicate the location of ECLs identified using the PG method for a given reanalysis, with no cyclones detected with the LAP method or in the MLDB. [Colour figure can be viewed at wileyonlinelibrary.com].

compared to 54% of all events. A larger proportion (25%) had mean rain rates in TRMM within 2.5° of the cyclone centre greater than 1 mm h^{-1}, equal to the proportion of all cyclones in MERRA. This highlights the challenges associated with attributing rainfall to cyclones, as much of the rain may be attributable to associated trough or front systems rather than the cyclone itself (Pepler *et al.,* 2014; Utsumi *et al.,* 2017). The mean radius of these cyclones is 1.9°, and none has a radius greater than 3.5°. However, these cyclones continue to have clear cyclonic winds in the CCMP observations, with rainfall concentrated to the south and east of the centre (Figure 11).

5. Discussion and conclusions

This paper follows Di Luca *et al.* (2015, 2016) to produce a comprehensive assessment of the representation of ECLs and their associated wind fields across four reanalyses – CFSR, ERAI, JRA55 and MERRA. These are evaluated in comparison to satellite observations of wind fields (CCMP) and rainfall (TRMM), as well as a subjective database of ECLs produced by Speer *et al.* (2009).

SLP in the MERRA reanalysis has a large amount of small-scale variability. Consequently, the number of cyclones identified from this reanalysis using a simple tracking scheme based on local minima of SLP is substantially higher than in a smoother reanalysis such as ERAI. A large number of these systems are very small lows on a surface trough without associated cyclonic winds, so can be comfortably excluded from analyses during post-processing of tracks. However, many other ECLs present in only the MERRA reanalysis have clear cyclonic characteristics in satellite wind and rain products.

The MERRA reanalysis produces lower central pressures and higher mean pressure differences for a given cyclone, further contributing to the differences between this reanalysis and ERAI. This is consistent with previous studies which identified a larger frequency of cyclones with very low central pressures and strong wind in the MERRA reanalysis using a range of cyclone identification methods (Hodges *et al.,* 2011; Tilinina *et al.,* 2013; Di Luca *et al.,* 2015; Wang *et al.,* 2016). The higher frequency

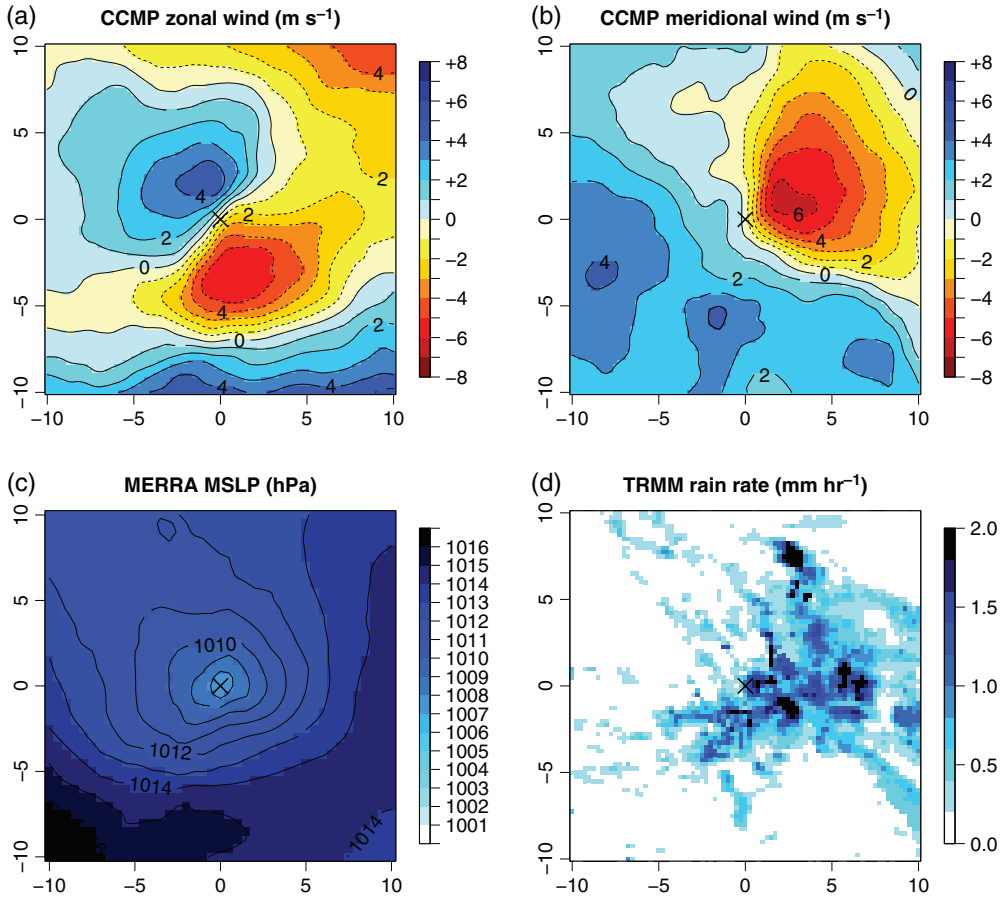

Figure 11. Composite (a) zonal and (b) meridional components of wind from CCMP within 10° for all ECLs in the MERRA reanalysis during 2007 that are identified by the PG method with *U*diff greater than 5 m s^{-1} but have no corresponding cyclone in any other dataset. (c) Mean SLP from MERRA reanalysis. (d) Mean TRMM rain rates. Dashed contours indicate negative values. [Colour figure can be viewed at wileyonlinelibrary.com].

of cyclones in MERRA was also identified for the northern hemisphere by Tilinina *et al.,* 2013; while this was not observed in Hodges *et al.,* 2011, this is likely due to the requirement for long-lived and mobile cyclones, which excludes the weaker and short-lived cyclones more common in MERRA.

The University of Melbourne (Murray and Simmonds, 1991; Simmonds *et al.,* 1999) tracking scheme incorporates improvements that reduce the frequency of erroneous cyclones generated along trough lines or topography. These improvements are sufficient to remove much of the differences between reanalyses and the small or non-cyclonic systems identified by simpler methods. The cyclones in PG-MERRA that are missing when identified using the LAP method tend to be small-scale systems, and are rarely associated with significant impacts, but have clear cyclonic circulation in the satellite wind fields and rainfall patterns typical of ECLs. Consequently, the LAP method may also be removing true small-scale systems, which is important to understand for studies that focus on such events.

The results from this paper suggest that the question of reanalysis choice may depend on the cyclone tracking method used:

- For a given set of ECLs, such as the Speer *et al.* (2009) database, ERAI consistently produces the most similar wind fields to the satellite data, followed closely by MERRA. Winds in CFSR consistently show the weakest relationship with the satellite data in southeast Australia across a range of metrics.
- When using a simple tracking scheme, ERAI produces the most realistic cyclones, and is less susceptible to erroneous small or non-cyclonic systems in trough lines or near the east coast. As ERAI also has the best representation of the CCMP wind fields, this is the generally recommended reanalysis.
- MERRA consistently produces more cyclones than other reanalyses, and is better able to represent small-scale or complex cyclones when compared to other reanalyses. However, while many of these additional systems are real ECLs, it also produces a large number of spurious lows. When using this method, substantial post-processing is required to exclude these. The more complex University of Melbourne cyclone tracking scheme is less susceptible to these pressure anomalies, at the expense of also excluding some genuine cyclones.
- No single reanalysis is a 'true' representation of the climate. Where possible, requiring a cyclone to be

identified by two different reanalyses, such as ERAI and MERRA, increases the likelihood of it being a true event. However, all reanalyses offer significant advantages over subjective databases, particularly in their ability to detect small, short-lived and rapidly developing events.

Acknowledgements

We acknowledge the helpful comments of two anonymous reviewers on an earlier draft of this manuscript. This research was supported by the Australian Research Council Linkage project grant LP120200777 and the Earth Systems and Climate Change hub of the Australian Government's National Environmental Science Programme.

References

Allen JT, Pezza AB, Black MT. 2010. Explosive cyclogenesis: a global climatology comparing multiple reanalyses. *J. Clim.* **23**(24): 6468–6484. https://doi.org/10.1175/2010JCLI3437.1.

Atlas R, Hoffman RN, Ardizzone J, Leidner SM, Jusem JC, Smith DK, Gombos D. 2010. A cross-calibrated, multiplatform ocean surface wind velocity product for meteorological and oceanographic applications. *Bull. Am. Meteorol. Soc.* **92**(2): 157–174. https://doi.org/10.1175/2010BAMS2946.1.

Browning SA, Goodwin ID. 2013. Large-scale influences on the evolution of winter subtropical maritime cyclones affecting Australia's east coast. *Mon. Weather Rev.* **141**(7): 2416–2431. https://doi.org/10.1175/MWR-D-12-00312.1.

Callaghan J, Helman P. 2008. Severe storms on the east coast of Australia, 1770-2008. Griffith Centre for Coastal Management, Griffith University, Gold Coast, Queensland, 240.

Callaghan J, Power SB. 2014. Major coastal flooding in southeastern Australia 1860–2012, associated deaths and weather systems. *Aust. Meteorol. Oceanogr. J.* **64**: 183–213.

Catto JL, Madonna E, Joos H, Rudeva I, Simmonds I. 2015. Global relationship between fronts and warm conveyor belts and the impact on extreme precipitation. *J. Clim.* **28**(21): 8411–8429. https://doi.org/10.1175/JCLI-D-15-0171.1.

Chang EKM, Lee S, Swanson KL. 2002. Storm track dynamics. *J. Clim.* **15**(16): 2163–2183. https://doi.org/10.1175/1520-0442(2002)015<02163:STD>2.0.CO;2.

Dee DP, Uppala SM, Simmons AJ, Berrisford P, Poli P, Kobayashi S, Andrae U, Balmaseda MA, Balsamo G, Bauer P, Bechtold P, Beljaars ACM, van de Berg L, Bidlot J, Bormann N, Delsol C, Dragani R, Fuentes M, Geer AJ, Haimberger L, Healy SB, Hersbach H, Hólm EV, Isaksen L, Kållberg P, Köhler M, Matricardi M, McNally AP, Monge-Sanz BM, Morcrette J-J, Park B-K, Peubey C, de Rosnay P, Tavolato C, Thépaut J-N, Vitart F. 2011. The ERA-Interim reanalysis: configuration and performance of the data assimilation system. *Q. J. R. Meteorol. Soc.* **137**(656): 553–597. https://doi.org/10.1002/qj.828.

Di Luca A, Evans JP, Pepler A, Alexander L, Argüeso D. 2015. Resolution sensitivity of cyclone climatology over eastern australia using six reanalysis products. *J. Clim.* **28**(24): 9530–9549. https://doi.org/10.1175/JCLI-D-14-00645.1.

Di Luca A, Evans JP, Pepler AS, Alexander LV, Argüeso D. 2016. Evaluating the representation of Australian East Coast Lows in a regional climate model ensemble. *J. Southern Hemisphere Earth Syst. Sci.* **66**: 108–124.

Dowdy AJ, Mills GA, Timbal B. 2013. Large-scale diagnostics of extratropical cyclogenesis in eastern Australia. *Int. J. Climatol.* **33**(10): 2318–2327. https://doi.org/10.1002/joc.3599.

Dowdy AJ, Mills GA, Timbal B, Wang Y. 2014. Fewer large waves projected for eastern Australia due to decreasing storminess. *Nat. Clim. Chang.* **4**: 283–286. https://doi.org/10.1038/nclimate2142.

Eichler TP, Gottschalck J. 2013. A comparison of southern hemisphere cyclone track climatology and interannual variability in coarse-gridded reanalysis datasets. *Adv. Meteorol.* **2013**: 891260. https://doi.org/10.1155/2013/891260.

Grieger J, Leckebusch GC, Donat MG, Schuster M, Ulbrich U. 2014. Southern Hemisphere winter cyclone activity under recent and future climate conditions in multi-model AOGCM simulations. *Int. J. Climatol.* **34**(12): 3400–3416. https://doi.org/10.1002/joc.3917.

Hodges KI, Lee RW, Bengtsson L. 2011. A comparison of extratropical cyclones in recent reanalyses ERA-Interim, NASA MERRA, NCEP CFSR, and JRA-25. *J. Clim.* **24**(18): 4888–4906. https://doi.org/10.1175/2011JCLI4097.1.

Holland GJ, Lynch AH, Leslie LM. 1987. Australian east-coast cyclones. part i: synoptic overview and case study. *Mon. Weather Rev.* **115**(12): 3024–3036. https://doi.org/10.1175/1520-0493(1987)115<3024:AECCPI>2.0.CO;2.

Hopkins LC, Holland GJ. 1997. Australian heavy-rain days and associated east coast cyclones: 1958-92. *J. Clim.* **10**(4): 621–635. https://doi.org/10.1175/1520-0442(1997)010<0621:AHRDAA>2.0.CO;2.

Huffman GJ, Bolvin DT, Nelkin EJ, Wolff DB, Adler RF, Gu G, Hong Y, Bowman KP, Stocker EF. 2007. The TRMM multisatellite precipitation analysis (TMPA): quasi-global, multiyear, combined-sensor precipitation estimates at fine scales. *J. Hydrometeorol.* **8**(1): 38–55. https://doi.org/10.1175/JHM560.1.

Irving D, Simmonds I, Keay K. 2010. Mesoscale cyclone activity over the ice-free southern ocean: 1999–2008. *J. Clim.* **23**(20): 5404–5420. https://doi.org/10.1175/2010JCLI3628.1.

Jones DA, Wang W, Fawcett R. 2009. High-quality spatial climate data-sets for Australia. *Aust. Meteorol. Oceanogr. J.* **58**(4): 233–248.

Kobayashi S, Ota Y, Harada Y, Ebita A, Moriya M, Onoda H, Onogi K, Kamahori H, Kobayashi C, Endo H, Miyaoka K, Takahashi K. 2015. The JRA-55 reanalysis: general specifications and basic characteristics. *J. Meteorol. Soc. Jpn. Ser. II* **93**(1): 5–48. https://doi.org/10.2151/jmsj.2015-001.

Leckebusch GC, Ulbrich U. 2004. On the relationship between cyclones and extreme windstorm events over Europe under climate change. *Glob. Planet. Chang.* **44**(1–4): 181–193. https://doi.org/10.1016/j.gloplacha.2004.06.011.

McInnes KL, Hubbert GD. 2001. The impact of eastern Australian cut-off lows on coastal sea levels. *Meteorol. Appl.* **8**(2): 229–243. https://doi.org/10.1017/S1350482701002110.

Murray RJ, Simmonds I. 1991. A numerical scheme for tracking cyclone centres from digital data. Part I: development and operation of the scheme. *Aust. Meteorol. Mag.* **39**(3): 155–166.

Neu U, Akperov MG, Bellenbaum N, Benestad R, Blender R, Caballero R, Cocozza A, Dacre HF, Feng Y, Fraedrich K, Grieger J, Gulev S, Hanley J, Hewson T, Inatsu M, Keay K, Kew SF, Kindem I, Leckebusch GC, Liberato MLR, Lionello P, Mokhov II, Pinto JG, Raible CC, Reale M, Rudeva I, Schuster M, Simmonds I, Sinclair M, Sprenger M, Tilinina ND, Trigo IF, Ulbrich S, Ulbrich U, Wang XL, Wernli H. 2013. IMILAST: a community effort to intercompare extratropical cyclone detection and tracking algorithms. *Bull. Am. Meteorol. Soc.* **94**(4): 529–547. https://doi.org/10.1175/BAMS-D-11-00154.1.

Papritz L, Pfahl S, Rudeva I, Simmonds I, Sodemann H, Wernli H. 2014. The role of extratropical cyclones and fronts for southern ocean freshwater fluxes. *J. Clim.* **27**(16): 6205–6224. https://doi.org/10.1175/JCLI-D-13-00409.1.

Pepler AS, Coutts-Smith A. 2013. A new, objective, database of East Coast Lows. *Aust. Meteorol. Oceanogr. J.* **63**(4): 461–472.

Pepler A, Coutts-Smith A, Timbal B. 2014. The role of East Coast Lows on rainfall patterns and inter-annual variability across the east coast of Australia. *Int. J. Climatol.* **34**(4): 1011–1021. https://doi.org/10.1002/joc.3741.

Pepler AS, Alexander LV, Evans JP, Sherwood SC. 2015a. Zonal winds and southeast Australian rainfall in global and regional climate models. *Clim. Dyn.* **46**: 123–133. https://doi.org/10.1007/s00382-015-2573-6.

Pepler AS, Di Luca A, Ji F, Alexander LV, Evans JP, Sherwood SC. 2015b. Impact of identification method on the inferred characteristics and variability of Australian East Coast Lows. *Mon. Weather Rev.* **143**(3): 864–877. https://doi.org/10.1175/MWR-D-14-00188.1.

Pepler AS, Di Luca A, Ji F, Alexander LV, Evans JP, Sherwood SC. 2016. Projected changes in east Australian midlatitude cyclones during the 21st century. *Geophys. Res. Lett.* **43**: 334–340. https://doi.org/10.1002/2015GL067267.

Pezza AB, Ambrizzi T. 2003. Variability of Southern Hemisphere cyclone and anticyclone behavior: further analysis. *J. Clim.* **16**(7): 1075–1083. https://doi.org/10.1175/1520-0442(2003)016<1075:VOSHCA>2.0.CO;2.

Pezza AB, Rashid HA, Simmonds I. 2012. Climate links and recent extremes in antarctic sea ice, high-latitude cyclones, Southern Annular

Mode and ENSO. *Clim. Dyn.* **38**(1-2): 57–73. https://doi.org/10.1007/s00382-011-1044-y.

Pfahl S, Wernli H. 2012. Quantifying the relevance of cyclones for precipitation extremes. *J. Clim.* **25**(19): 6770–6780. https://doi.org/10.1175/JCLI-D-11-00705.1.

Pinto JG, Spangehl T, Ulbrich U, Speth P. 2005. Sensitivities of a cyclone detection and tracking algorithm: individual tracks and climatology. *Meteorol. Z.* **14**(6): 823–838. https://doi.org/10.1127/0941-2948/2005/0068.

Rienecker MM, Suarez MJ, Gelaro R, Todling R, Bacmeister J, Liu E, Bosilovich MG, Schubert SD, Takacs L, Kim G-K, Bloom S, Chen J, Collins D, Conaty A, da Silva A, Gu W, Joiner J, Koster RD, Lucchesi R, Molod A, Owens T, Pawson S, Pegion P, Redder CR, Reichle R, Robertson FR, Ruddick AG, Sienkiewicz M, Woollen J. 2011. MERRA: NASA's modern-era retrospective analysis for research and applications. *J. Clim.* **24**(14): 3624–3648. https://doi.org/10.1175/JCLI-D-11-00015.1.

Rudeva I, Gulev SK. 2007. Climatology of cyclone size characteristics and their changes during the cyclone life cycle. *Mon. Weather Rev.* **135**(7): 2568–2587. https://doi.org/10.1175/MWR3420.1.

Saha S, Moorthi S, Pan H-L, Wu X, Wang J, Nadiga S, Tripp P, Kistler R, Woollen J, Behringer D, Liu H, Stokes D, Grumbine R, Gayno G, Wang J, Hou Y-T, Chuang H-Y, Juang H-MH, Sela J, Iredell M, Treadon R, Kleist D, Van Delst P, Keyser D, Derber J, Ek M, Meng J, Wei H, Yang R, Lord S, Van Den Dool H, Kumar A, Wang W, Long C, Chelliah M, Xue Y, Huang B, Schemm J-K, Ebisuzaki W, Lin R, Xie P, Chen M, Zhou S, Higgins W, Zou C-Z, Liu Q, Chen Y, Han Y, Cucurull L, Reynolds RW, Rutledge G, Goldberg M. 2010. The NCEP climate forecast system reanalysis. *Bull. Am. Meteorol. Soc.* **91**(8): 1015–1057. https://doi.org/10.1175/2010BAMS3001.1.

Simmonds I, Murray RJ. 1999. Southern extratropical cyclone behavior in ECMWF analyses during the FROST special observing periods. *Weather Forecast.* **14**(6): 878–891. https://doi.org/10.1175/1520-0434(1999)014<0878:SECBIE>2.0.CO;2.

Simmonds I, Murray RJ, Leighton RM. 1999. A refinement of cyclone tracking methods with data from FROST. *Aust. Meteorol. Mag.* (special edition): 35–49.

Speer MS, Wiles P, Pepler A. 2009. Low pressure systems off the New South Wales coast and associated hazardous weather: establishment of a database. *Aust. Meteorol. Oceanogr. J.* **58**(1): 29–39.

Tilinina N, Gulev SK, Rudeva I, Koltermann P. 2013. Comparing cyclone life cycle characteristics and their interannual variability in different reanalyses. *J. Clim.* **26**(17): 6419–6438. https://doi.org/10.1175/JCLI-D-12-00777.1.

Timbal B, Drosdowsky W. 2013. The relationship between the decline of Southeastern Australian rainfall and the strengthening of the subtropical ridge. *Int. J. Climatol.* **33**(4): 1021–1034. https://doi.org/10.1002/joc.3492.

Utsumi N, Kim H, Kanae S, Oki T. 2017. Relative contributions of weather systems to mean and extreme global precipitation. *J. Geophys. Res. Atmos.* **122**: 152–167. https://doi.org/10.1002/2016JD025222.

Wang XL, Feng Y, Chan R, Isaac V. 2016. Inter-comparison of extra-tropical cyclone activity in nine reanalysis datasets. *Atmos. Res.* **181**: 133–153. https://doi.org/10.1016/j.atmosres.2016.06.010.

